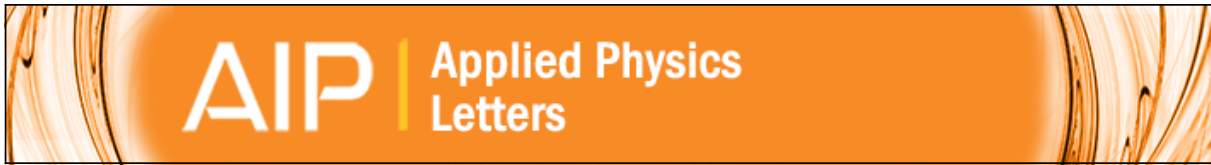




Title	Indium tin oxide and indium phosphide heterojunction nanowire array solar cells
Author(s)	Yoshimura, Masatoshi; Nakai, Eiji; Tomioka, Katsuhiro; Fukui, Takashi
Citation	Applied Physics Letters, 103(24), 243111 https://doi.org/10.1063/1.4847355
Issue Date	2013-12-09
Doc URL	http://hdl.handle.net/2115/54804
Rights	Copyright 2013 American Institute of Physics. This article may be downloaded for personal use only. Any other use requires prior permission of the author and the American Institute of Physics. The following article appeared in Appl. Phys. Lett. 103, 243111(2013) and may be found at http://scitation.aip.org/content/aip/journal/apl/103/24/10.1063/1.4847355/
Type	article
File Information	APL103-24_243111.pdf



[Instructions for use](#)



Indium tin oxide and indium phosphide heterojunction nanowire array solar cells

Masatoshi Yoshimura, Eiji Nakai, Katsuhiro Tomioka, and Takashi Fukui

Citation: [Applied Physics Letters](#) **103**, 243111 (2013); doi: 10.1063/1.4847355

View online: <http://dx.doi.org/10.1063/1.4847355>

View Table of Contents: <http://scitation.aip.org/content/aip/journal/apl/103/24?ver=pdfcov>

Published by the [AIP Publishing](#)



Re-register for Table of Content Alerts

Create a profile.



Sign up today!



Indium tin oxide and indium phosphide heterojunction nanowire array solar cells

Masatoshi Yoshimura,^{1,a)} Eiji Nakai,¹ Katsuhiko Tomioka,^{1,2} and Takashi Fukui¹

¹Graduate School of Information Science and Technology, and Research Center for Integrated Quantum Electronics (RCIQE), Hokkaido University, Kita 13 Nishi 8, Sapporo 060–8628, Japan

²PRESTO, Japan Science and Technology Agency (JST), Honcho Kawaguchi, 332–0012 Saitama, Japan

(Received 22 October 2013; accepted 27 November 2013; published online 12 December 2013)

Heterojunction solar cells were formed with a position-controlled InP nanowire array sputtered with indium tin oxide (ITO). The ITO not only acted as a transparent electrode but also as forming a photovoltaic junction. The devices exhibited an open-circuit voltage of 0.436 V, short-circuit current of 24.8 mA/cm², and fill factor of 0.682, giving a power conversion efficiency of 7.37% under AM1.5G illumination. The internal quantum efficiency of the device was higher than that of the world-record InP cell in the short wavelength range. © 2013 AIP Publishing LLC. [<http://dx.doi.org/10.1063/1.4847355>]

Photovoltaic devices based on semiconductor nanowire (NW) arrays have drawn interest as a possible way of reducing costs and materials while maintaining the power conversion efficiency of solar cells.^{1–8} A size- and position-optimized array of NWs can absorb an amount of light almost equal to that of a bulk structure with an antireflection coating because of its near-field-optics enhanced absorption and anti-reflection effect.^{9,10} However, photovoltaics based on NW arrays need to have a transparent electrode put on their NWs before the collecting electrode is formed, because each NW independently functions as a solar cell. In many cases, indium tin oxide (ITO) has been used as the transparent electrode since it has high conductivity and transmittance.^{1–7,11} We have focused on the ITO because it can act not only as a transparent conductive oxide but also as forming a photovoltaic junction with groups IV and III-V semiconductors.^{12–14} In particular, it has been reported that an ITO/InP planar solar cells have a power conversion efficiency of 18.9%.¹⁴ This suggests the possibility of making less costly ITO/NW-array heterojunction solar cells that require only a single-doped NW array. Moreover, the use of one doped NW growth layer instead of two would give us more control over the crystal growth conditions.¹⁵

In this study, we experimentally demonstrated an ITO/InP heterojunction NW array photovoltaic device. The *p*-doped InP NW array was epitaxially grown using selective area growth (SAG), which has the capability of position control. Photovoltaic junctions were formed by ITO sputtering on the *p*-InP NW array. The resulting heterojunction NW-array cell had low reflectance and excellent quantum efficiency in the short wavelength region.

The NW growth and the fabrication process for the NW array solar cells were as previously reported.¹⁶ We grew *p*-type InP NWs by selective-area MOVPE using a 20-nm-thick SiO₂ mask deposited onto *p*-type InP (111)A substrates ($N_A \sim 5 \times 10^{18} \text{ cm}^{-3}$). The SiO₂ pattern was designed to be a triangular periodic array of openings with a diameter, d_0 , of 200 nm and pitch, a , of 400 nm in $1.2 \times 1.2 \text{ mm}^2$ regions. The NWs were grown using metal-organic vapor phase

epitaxy. After the growth, the NW array was embedded by spin-coating benzocyclobutene (BCB, Dow Chemical). The BCB layer was etched by reactive ion etching (RIE) with CF₄/O₂, exposing the tips of the NWs. A transparent ITO (SnO₂/In₂O₃ 10:90 wt. %) layer was then rf sputtered at a rate of 1.1 Å/s for 45 min onto the NW array at room temperature and annealed in N₂ at 400 °C for 15 min. The sputtered ITO film typically has a sheet resistance of 10 Ω/□ and an optical transmittance higher than 85% in the wavelength range between 400 nm and 900 nm. U-shaped Ag and alloying Au-Zn electrodes were, respectively, formed on the ITO layer and back of the substrate. The active device area was 0.62 mm² and included approximately 4.5×10^6 NWs.

Figure 1(a) shows 20°-tilted scanning electron microscopy (SEM) image of *p*-InP NWs grown on patterned *p*-InP(111)A substrates. The NWs were well-defined and highly uniform in length, diameter, shape, and position. The sidewalls of the hexagonal NW were {−211} facet surfaces vertical to the substrate, as shown in Fig. 1(b). The average height and diameter of NWs were 1.0 μm and 170 nm, respectively. The geometric fill factor (FF), i.e., the ratio between the footprint area of the NW and the area of the unit cell, was 18%. The SEM image in Fig. 1(c) shows a cross-section of the NWs after completion of the device processes. The sputtered ITO layer had a dome-shaped morphology, which functioned as a light coupling within the NW array.¹⁷

Figure 2(a) shows the current density versus voltage (*J*–*V*) characteristics of the fabricated ITO/*p*-InP heterojunction solar cell. They were measured under AM1.5G (1 sun) illumination at 25.0 °C. The illumination intensity was calibrated using a standard silicon photodiode (Bunkoukeiki BS-500). The inset shows the *J*–*V* characteristics of the cell in the dark. The device had good rectifying properties and a rectification ratio greater than 10⁴ at ±1.0 V in the dark, which means that a photovoltaic junction formed in it. These rectification properties can be attributed to SAG, which guarantees high crystal quality by preventing any metal from being incorporated during epitaxial growth.¹⁸ There are several models that could be used to explain the behavior of the ITO/*p*-InP junction, including heterostructure, buried *n*⁺/*p* homojunction,¹⁹ metal-insulator-semiconductor,²⁰ and

^{a)}yoshimura@rciqe.hokudai.ac.jp.

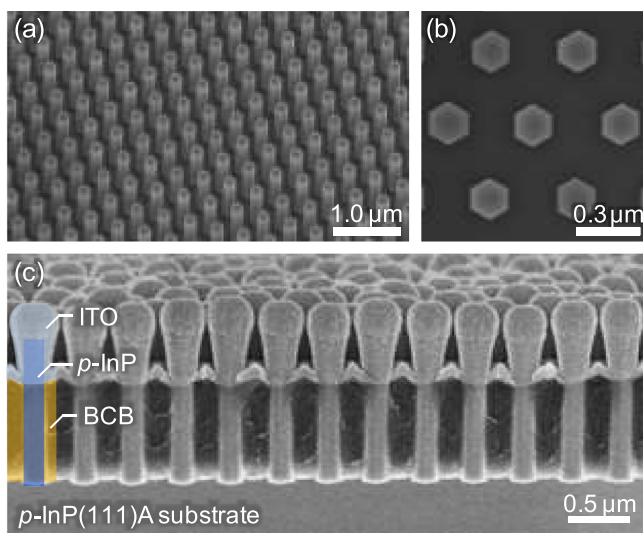


FIG. 1. (a) 20°-tilted view SEM image of *p*-InP NW array. (b) A top view SEM image of the NWs. (c) Cross-sectional SEM image of ITO/*p*-InP heterojunction NW solar cell.

metal-semi-insulating-semiconductor,²¹ but the buried n^+/p homojunction model is compelling because the deposition of an ITO layer induces an n^+ -defect layer near the surface.¹⁹

The device exhibited an open circuit voltage (V_{OC}) of 0.436 V, a short circuit current density (J_{SC}) of 24.8 mA/cm², and a FF of 0.682, for an overall power conversion efficiency (η) of 7.37%. The current density and efficiency were determined from the active area, 82% of which was the space between the NWs. This high J_{SC} for a NW-array-based device resulted from the combination of near-field-optics enhanced absorption and anti-reflection effects.¹⁰ The ideality factor and series resistance determined from the illuminated J - V characteristics²² were 1.6 and 0.21 Ω ·cm².

To analyze the absorption properties, we investigated the quantum efficiency of the heterojunction cell, as shown in Fig. 2(b). In the wavelength range between 370 nm and 730 nm, the internal quantum efficiency (IQE) of the device exceeded 80%, despite the device covering only 18% of the substrate surface. The IQE at shorter wavelengths was much higher than the previous reported InP NW solar cell,¹⁶ and the device had peak IQE of 0.943 at 490 nm without employing a window layer for reflecting minority carriers moving toward the front ITO layer. Moreover, the IQE of our heterojunction cell was significantly greater than that of the current world record holder for InP planar cells²³ in the range of 300 nm and 570 nm. There were two reasons for this. First,

the wide-band-gap ITO layer functioned as a window layer, which reflects minority carriers, for the InP layer; thus, IQE increased because of a reduction in the amount of surface recombination. Second, the tips of the InP NWs, whose average length was 300 nm, were covered by hemispherical caps of ITO. A photovoltaic junction formed not only at the top but also on the sides of the NWs, and this resulted in an improvement in the separation and collection efficiency of the photogenerated carriers. In addition, more than 98% of the incident light with wavelengths less than 500 nm was absorbed within a depth of 300 nm in the InP, and hence, the IQE at shorter wavelengths increased. The effective reflectance of the device after taking account of the solar spectrum distribution²⁴ was 6.2%, and it should be emphasized that the device did not have specially designed antireflection coatings. It is thought the lower index of refraction in the NW array structure made for a stepped-index antireflection coating.²⁵ In addition, the ITO layer had a high-refractive index ($n \sim 1.95$) and suppressed scattering of light.

The absorption on the low-energy side started to rise from about 870 nm, which is substantially blue-shifted relative to the bulk bandgap of InP (925 nm). To examine the course of the blue-shift, we measured the crystal structure of the InP NW by using high-resolution transmission electron microscopy (HR-TEM) at an acceleration voltage of 300 kV along the $\langle -110 \rangle$ incidence, as shown in Fig. 3(a). Figures 3(b) and 3(c) show the corresponding selective area electron diffraction (SAED) patterns. In the HR-TEM image, the crystal structure in the NW region is clearly different from the substrate region. The SAED pattern at the NW indicates the grown *p*-InP NW is a pure wurtzite structure without a zincblende structure (Fig. 3(b)); in contrast, zincblende spots can be seen in the SAED pattern at the interface between the NWs and the substrate (Fig. 3(c)). The wurtzite structure of the NWs was confirmed by making a reciprocal space mapping results of X-ray diffraction, as shown in Fig. 3(d). The (10–1.5) and (331) peaks correspond to wurtzite and zincblende structures. This is consistent with our previous results whose samples were grown under similar growth-temperature and V/III ratio conditions.²⁶ It is known that bandgap energy of wurtzite InP is about 80 meV higher than that of zincblende.²⁷ This suggests that the absorption edge on the low-energy side of the heterojunction device is blue-shifted. To clarify the bandgap shift in the *p*-InP NWs, the wires were studied with micro-photoluminescence (PL) at room temperature (Fig. 3(e)). The PL spectrum of the InP substrate exhibits a peak at 920 nm (=1.35 eV), while the

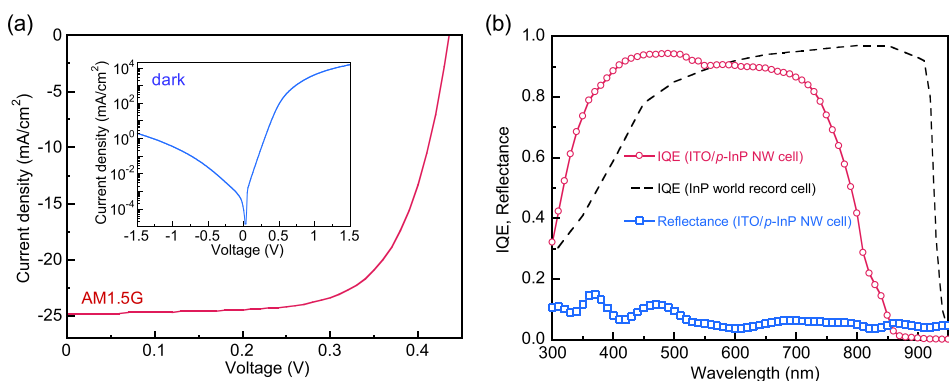


FIG. 2. (a) Illuminated J - V characteristics of the ITO/*p*-InP NW cell under AM1.5G. Inset shows dark J - V characteristics (semilog scale). (b) Internal quantum efficiency and reflectance of ITO/*p*-InP NW cell. It is compared with the IQE of the InP-world record planar cell reported in Ref. 23.

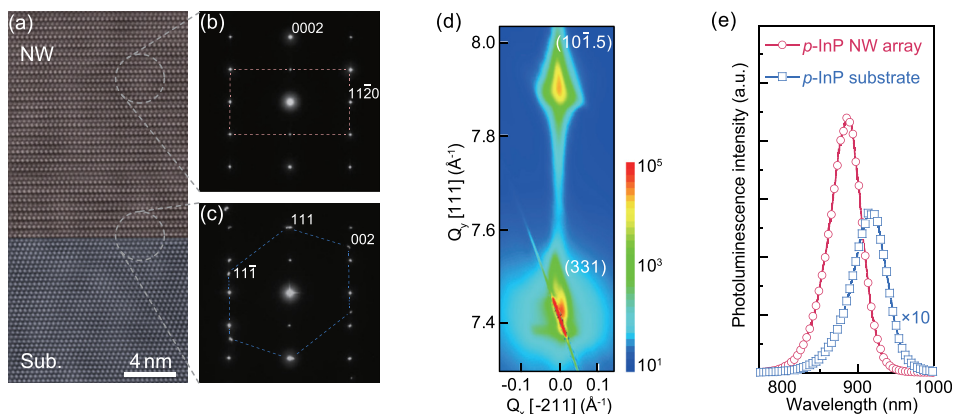


FIG. 3. (a) HR-TEM image for a *p*-InP NW/substrate interface. The corresponding SAED patterns at the (b) NW and (c) NW/substrate interfaces. Incident direction of electron beam is $\langle -110 \rangle$. (d) Reciprocal space mapping for the *p*-InP NW on the substrate. (e) PL spectra for *p*-InP NWs and *p*-InP substrate at room temperature.

spectrum of the *p*-InP NWs had a peak at 885 nm ($=1.40$ eV). The PL peak of the NWs was blue-shifted, but it was less than the theoretical predicted 80 meV. This could be explained by the free-to-bound excitons stemming from zinc-doping. In addition, the HR-TEM image shows that the *p*-InP NWs had no twin and misfit dislocations, suggesting that the grown NWs were high-quality wurtzite crystals. This resulting low rate of bulk recombination was another source of IQE improvement.

In conclusion, we demonstrated a heterojunction solar cell that combines a *p*-doped InP NW array and a transparent ITO layer. The position-controlled and catalyst-free NWs were grown using SAG. The fabricated device showed a power conversion efficiency of 7.37% under AM1.5G with a J_{SC} of 24.8 mA/cm². Furthermore, the ITO/InP heterojunction cell showed higher IQE than that of the current world-record-holding InP cell in the wavelength range below 570 nm. This approach of using transparent ITO film not only for electrically connecting the NWs in parallel but also for forming a photovoltaic junction has great potential in NW-based solar cells.

The authors thank J. Motohisa and S. Hara for valuable discussions. This work was financially supported by a Grant-in-Aid Scientific Research from the Ministry of Education, Culture, Sports, Science and Technology (MEXT) Grant No. 23221007.

¹H. Goto, K. Nosaki, K. Tomioka, S. Hara, K. Hiruma, J. Motohisa, and T. Fukui, *Appl. Phys. Express* **2**, 035004 (2009).

²J. Wallentin, N. Anttu, D. Asoli, M. Huffman, I. Aberg, M. H. Magnusson, G. Siefert, P. Fuss-Kailuweit, F. Dimroth, B. Witzigmann, H. Q. Xu, L. Samuelson, K. Deppert, and M. T. Borgstrom, *Science* **339**, 1057 (2013).

³G. Mariani, A. C. Scofield, C.-H. Hung, and D. L. Huffaker, *Nat. Commun.* **4**, 1497 (2013).

⁴P. Krogstrup, H. I. Jorgensen, M. Heiss, O. Demichel, J. V. Holm, M. Aagesen, J. Nygard, and A. F. i. Morral, *Nat. Photonics* **7**, 306 (2013).

⁵G. Mariani, P.-S. Wong, A. M. Katzenmeyer, F. Léonard, J. Shapiro, D. L. Huffaker, and L. Francois, *Nano Lett.* **11**, 2490 (2011).

⁶Y. Cui, J. Wang, S. R. Plissard, A. Cavalli, T. T. T. Vu, R. P. J. V. Veldhoven, L. Gao, M. Trainor, M. A. Verheijen, J. E. M. Haverkort, and E. P. A. M. Bakkers, *Nano Lett.* **13**, 4113 (2013).

⁷J. C. Shin, K. H. Kim, K. J. Yu, H. Hu, L. Yin, C.-Z. Ning, J. A. Rogers, J.-M. Zuo, and X. Li, *Nano Lett.* **11**, 4831 (2011).

⁸J. V. Holm, H. I. Jorgensen, P. Krogstrup, J. Nygard, H. Liu, and M. Aagesen, *Nat. Commun.* **4**, 1498 (2013).

⁹L. Hu and G. Chen, *Nano Lett.* **7**, 3249 (2007).

¹⁰J. Kupec, R. L. Stoop, and B. Witzigmann, *Opt. Express* **18**, 27589–27605 (2010).

¹¹T. Fukui, M. Yoshimura, E. Nakai, and K. Tomioka, *Ambio* **41**, 119 (2012).

¹²N. Inoue, T. Miyakawa, and C. W. Wilmsen, *Jpn. J. Appl. Phys.* **20**(Suppl. 20-2), 11 (1981), <http://jap.jp/link?JJAPS/20S2/11>.

¹³P. Sheldon and R. Hayes, *J. Vac. Sci. Technol.* **20**, 410 (1982).

¹⁴X. Li, M. Wanlass, and T. Gessert, *Appl. Phys. Lett.* **54**, 2674 (1989).

¹⁵M. T. Borgström, E. Norberg, P. Wickert, H. A. Nilsson, J. Trägårdh, K. A. Dick, G. Statkute, P. Ramvall, K. Deppert, and L. Samuelson, *Nanotechnology* **19**, 445602 (2008).

¹⁶M. Yoshimura, E. Nakai, K. Tomioka, and T. Fukui, *Appl. Phys. Express* **6**, 052301 (2013).

¹⁷G. Mariani, Z. Zhou, A. Scofield, and D. L. Huffaker, *Nano Lett.* **13**, 1632 (2013).

¹⁸J. Jackson and D. Kapoor, *J. Appl. Phys.* **102**, 054310 (2007).

¹⁹J. K. Luo and H. Thomas, *J. Electron. Mater.* **22**, 1311 (1993).

²⁰R. Singh and J. Shewchun, *J. Appl. Phys.* **49**, 4588 (1978).

²¹P. Sheldon, R. K. Ahrenkiel, R. E. Hayes, and P. E. Russell, *Appl. Phys. Lett.* **41**, 727 (1982).

²²K. Ishibashi, Y. Kimura, and M. Niwano, *J. Appl. Phys.* **103**, 094507 (2008).

²³C. J. Keavney, V. E. Haven, and S. M. Vernon, in *Proceedings of 21st IEEE Photovoltaic Specialists Conference* (1990), p. 141.

²⁴S. Strehlke, S. Bastide, and C. Le, *Sol. Energy Mater. Sol. Cells* **58**, 399 (1999).

²⁵O. Muskens, J. Rivas, and R. Algra, *Nano Lett.* **8**, 2638 (2008).

²⁶P. Mohan, J. Motohisa, and T. Fukui, *Nanotechnology* **16**, 2903 (2005).

²⁷M. Murayama and T. Nakayama, *Phys. Rev. B* **49**, 4710 (1994).